# A compact double-pass Raman backscattering amplifier/compressor[a)]

J. Ren,[1,b)] S. Li,[1] A. Morozov,[1] S. Suckewer,[1] N. A. Yampolsky,[2] V. M. Malkin,[2] and N. J. Fisch[2]
[1]*Department of Mechanical and Aerospace Engineering, Princeton University, Princeton, New Jersey 08544, USA*
[2]*Department of Astrophysical Sciences, Princeton University, Princeton, New Jersey 08544, USA*

(Received 19 December 2007; accepted 22 January 2008; published online 6 March 2008)

The enhancement of stimulated Raman backscattering (SRBS) amplification was demonstrated by introducing a plasma density gradient along the pump and the seed interaction path and by a novel double-pass design. The energy transfer efficiency was significantly improved to a level of 6.4%. The seed pulse was amplified by a factor of more than 20 000 from the input in a 2 mm long plasma, which also exceeded the intensity of the pump pulse by 2 orders of magnitude. This was accompanied by very effective pulse compression, from 500 fs to 90 fs in the first pass measurements and in the second pass down to approximately 50 fs, as it is indicated by the energy-pulse duration relation. Further improvements to the energy transfer efficiency and the SRBS performance by extending the region of resonance is also discussed where a uniform ~4 mm long plasma channel for SRBS was generated by using two subsequent laser pulses in an ethane gas jet. © *2008 American Institute of Physics*. [DOI: 10.1063/1.2844352]

## I. INTRODUCTION

After 40 years of laser research and development, the focus today is on developing high-power, compact lasers.[1–3] Advances in laser power and reductions in system size and cost continue to foster exploration in many areas of science and engineering, including particle accelerators in plasma,[4] fast laser ignition in fusion-energy production,[5] x-ray lasers,[6] as well as in medical sciences that also benefit from the development of ultraintense and ultrashort pulse sources.[7] Currently, most high power, ultrashort pulse lasers depend on the chirped-pulse-amplification (CPA) method,[8] in which a short laser pulse is stretched to avoid damaging an amplifying medium and then compressed after amplification. High power lasers require large, expensive gratings to control the nonlinear effects at power levels above $GW/cm^2$ along with the requirement for uniform amplification over a broad bandwidth, which is both difficult and challenging.

Using plasma, which can tolerate much higher radiation intensity, as the amplifying medium, overcomes such limitations. More specifically, it was proposed that in plasma a resonant interaction could be arranged between two counterpropagating electromagnetic waves, known as pump and seed waves, which would excite a plasma wave, and which would also convert the energy of the long pump pulse into the much shorter seed pulse.[9] The output beam should undergo simultaneous amplification and compression; moreover, since plasma is impervious to optical damage, the power can grow to extraordinary levels.[9,10] In fact, this resonant stimulated Raman backscattering (SRBS) amplifier has been shown to be successful and very promising,[11–14] where the input pulse is amplified through a plasma-mediated three-wave interaction and resonance, with the resonance condition requirement,

$$\omega_{\text{pump}} = \omega_{\text{seed}} + \omega_{pe}, \tag{1}$$

$\omega_{\text{pump}}$, $\omega_{\text{seed}}$, and $\omega_{pe}$ are frequencies of the pump, the seed, and the plasma wave, respectively. Very high output intensities, i.e., as much as $2\times10^{17}$ $W/cm^2$ from an unfocused output pulse,[9] ought to be obtainable through such a scheme, compared to the only a few $GW/cm^2$ power levels achieved in a normal optical amplifying medium. The maximum energy ratio transferred from the pump to the seed is proportional to the ratio of their frequencies, and with $\omega_{\text{pump}} \geqslant 10\omega_{pe}$ the energy transfer efficiency can be as high as 90%. Computational studies supported the conclusion that a window in parameter space exists wherein the theoretical efficiencies should be attainable.[15] However, the efficiencies that were demonstrated by experiment are much lower than the theoretical limit[9,10] reaching about 1% in Ref. 12 which makes the applications of this ultrahigh power laser far from being practical.

One possible explanation of the nonideal amplification comes from the procedure of lengthening the pump pulse duration from its maximum compression (100 fs, minimum chirp), to the desired pulse length of ~20 ps by moving the gratings away from the nonchirp position, hence increasing the chirp. The frequency and spectral detuning of the pump pulse with its bandwidth $\Delta\lambda_{\text{pump}}=12$ nm (800 nm center wavelength) is estimated as $\Delta\omega_{\text{pump}}/\omega_{\text{pump}}=\Delta\lambda_{\text{pump}}/\lambda_{\text{pump}}=12/800=1.5\%$. The bandwidth of the amplified seed pulse also increases during the amplification[12] and large bandwidths of the pump and the seed pulses result in breaking down the resonant interaction between the waves since the resonant condition equation (1) is not exactly satisfied. An increased bandwidth of the plasma wave along the path of the interaction can enhance coupling between the waves and thus produce increased output seed energy.[16] The Raman

[a)]Paper CI1 5, Bull. Am. Phys. Soc. **52**, 59 (2007).
[b)]Invited speaker.

 

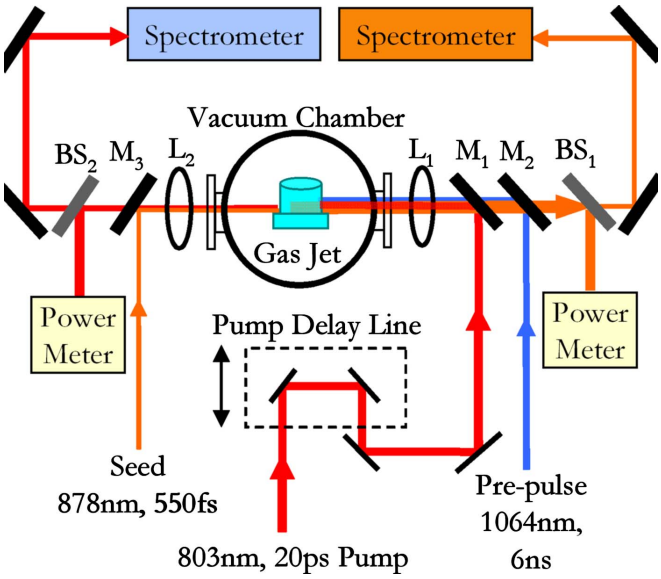


FIG. 1. (Color online) Schematic diagram of the experimental setup. $M_1$, $M_2$, and $M_3$ are reflecting mirrors for pump, prepulse, and seed, respectively. $L_1$ and $L_2$ are the focusing lens and $BS_1$ and $BS_2$ are beamsplitters.

backscattering coupling has been simulated in the inhomogeneous plasma, where the propagation and amplification is along the selected plasma channel.[17] However, the resonant interaction is known to be changed in a density gradient.[18] Currently, this possibility is under further theoretical study.[19]

To further improve the efficiency of the SRBS, we noticed that even for large amplification and compression, only a small fraction of the total pump energy was being used, and about 80%–85% of the initial pump energy was passing through the 2 mm plasma. Therefore our solution was to reflect the "unused" portion of the pump energy back to the plasma while simultaneously reflecting back the already amplified seed pulse and having them interact again in the same plasma for a second round of amplification.

## II. EXPERIMENT AND RESULTS

### A. The first pass

Figure 1 shows the schematic diagram of our experimental setup for the first pass amplification. A gas nozzle ejects ethane ($C_2H_6$) gas and forms a gas jet, a ND:YAG laser pulse (called the "prepulse") with wavelength 1.064 $\mu$m, pulse duration ~6 ns, focused spot size diameter ~50 $\mu$m, pulse energy ~500 mJ, and pulse intensity $\sim 4\times10^{12}$ W/cm$^2$ ionizes the gas jet and produces the plasma channel. The pump and the seed pulses were created from splitting the uncompressed output of a Ti:sapphire laser system (central wavelength 803 nm, with a bandwidth of ~12 nm and FWHM of pulse duration ~240 ps): 95% compressed to ~20 ps with preserved original bandwidth was used as the pump; the rest, 5%, was sent to a 7 cm long barium nitride Raman crystal. The first stoke beam generated in the crystal with a central wavelength of 878 nm, and a slightly narrowed bandwidth of ~9 nm was compressed by a separate compressor to ~500 fs and used as the seed. In the experiment, the long pumping pulse propagates along the plasma channel from the right and meets the short seed pulse injected from the left, and through SRBS amplifies the input seed pulse. After amplification, the seed pulse spectrum, energy and pulse duration were measured, respectively, with a spectrometer, power meter and autocorrelator (not shown in Fig. 1).

The temporal overlap between the pump and the seed was achieved by overlapping the pump and the seed cross signal in a second-harmonic-generation (SHG) crystal, and then fine-tuning the overlap with the pump delay stage by looking for the maximum amplification during the experiment. The spatial overlap was first obtained by using diagnostic and imaging systems which consisted of two He–Ne beams, alignment optics and a CCD camera.

The plasma density profile had a plateau of a median value $\sim 1.3\times10^{19}$ cm$^{-3}$ (within $\pm$10% variation) on its axis, and an increasing density along the radial direction due to expansion of the plasma channel. Radially, the plasma density reached the maximum value of $\sim 2.2\times10^{19}$ cm$^{-3}$ at a distance of 75 $\mu$m then dropped to $\sim 0.6\times10^{19}$ cm$^{-3}$ at a distance of 125 $\mu$m, bringing a channel size of ~250 $\mu$m in diameter.[20] Therefore, by letting the beam go slightly "off axis," a plasma density gradient was introduced along the pump seed interaction path. Taking into account that the laser pulse propagating through the plasma in off-axis geometry is changing its direction due to the plasma refraction, in the experiment the optimal pump direction and path in the plasma channel was adjusted. The seed beam direction and path was modified accordingly (with seed reflecting mirror $M_3$) to ensure its best overlap with the pump for the optimal Raman backscattering amplification. The optimal Raman backscattering amplification was indicated by the maximum gain and the widest amplified seed spectrum therefore the shortest amplified seed pulse duration. We found that the optimal tilted angle of the pump beams was ~5°, which was significantly larger than the calculated critical angle of the beam that can be guided by the channel density profile (<2°). Nevertheless, we observed that pump beam was channeling quite well in the plasma and was nearly parallel to the plasma axis at its exit.

A summary of the results of the pulse amplification and compression from the first pass of SRBS are shown in Figs. 2(a)–2(h). In Fig. 2(a) the output pulse energy is shown to increase with the pumping energy, and energy gain from the input reaches ~240 at the maximum output energy of ~3.6 mJ for the input seed energy ~16 $\mu$J. The energy conversion efficiency from the pump to the seed is shown in Fig. 2(b), and reaches about 4% at the pumping energy of ~60 mJ.

The compression of the amplified pulse in plasma is shown in Figs. 2(c)–2(f). Figures 2(c) and 2(d) show that the measured seed spectrum increases from ~9 nm before amplification to ~32 nm after the amplification (the amplified pulse having an energy of ~3.6 mJ). The broadening of the seed pulse spectrum is consistent with the pulse duration shortening in Figs. 2(e) and 2(f), where the seed pulse time profile, measured with an autocorrelator, is shown to decrease from ~500 fs at the input to ~90 fs at the output (the amplified pulse having an energy of ~2.9 mJ). Assuming the

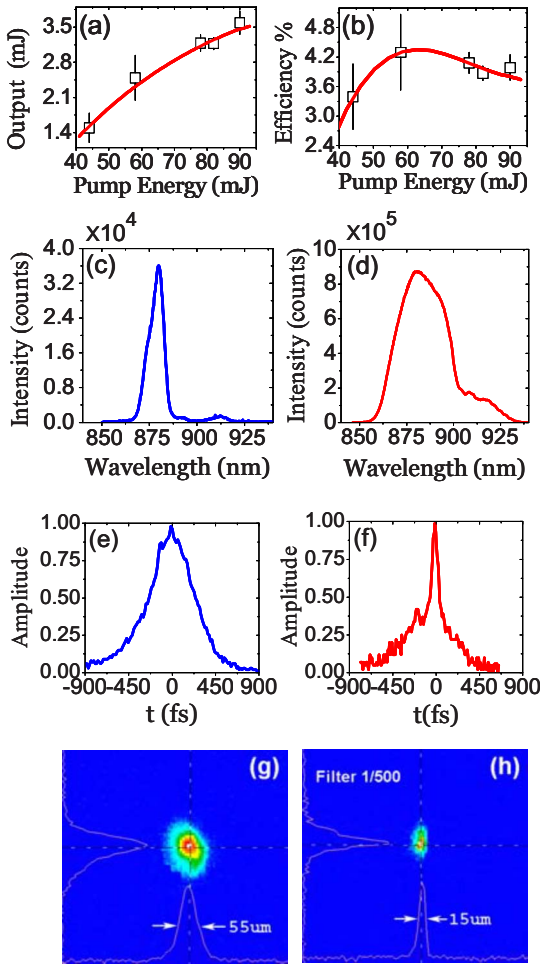


FIG. 2. (Color online) Summary of pulse amplification and compression in the first pass with the input seed pulse energy ~16 $\mu$J, including the amplified output pulse energy versus the pumping energy in (a) and energy conversion efficiency from pump to seed in (b); spectrum broadening from 9 nm of the input pulse (c) to ~32 nm of the output pulse with ~3.6 mJ amplified energy (d); pulse compression from ~500 fs of the input pulse (e) to ~90 fs of the output pulse with ~2.9 mJ amplified energy (f); and the spatial profile of the seed before (g) and after (h) amplification.

compressed pulse has a $\pi$-pulse shape where the main spike is followed by a spike train of smaller amplitude, in the self-similar coordinate the location $z_M$ of the spike and the spike amplitude $A$ is given by[9,10]

$$z_M = \ln \frac{4\sqrt{2\pi \times z_M}}{\varepsilon},$$

$$A = \frac{z_M}{\sqrt{2\xi \times \sqrt{\omega\omega_{pe}}}},$$

$$\xi = x/c + t, \tag{2}$$

$$\xi_M = z_M^2/4\tau,$$

$$\tau = \frac{t}{2}\omega\omega_{pe}a_0^2.$$

Here $\varepsilon$ is the integrated amplitude of the input seed, $\omega$ and $\omega_{pe}$ are the frequency of the pump and plasma, respectively, and $a_0$ is the normalized vector potential of the pump. Curve fitting Eq. (2) with our measured autocorrelator results showed that the leading first spike contains about 50% of the total energy.

The spatial profile of the seed pulse before and after the amplification is shown in Figs. 2(g) and 2(h). Images were obtained at the right side of the plasma end in Fig. 1, where the amplified pulse leaves the plasma. Figure 2(g) shows the input seed with the FWHM of the beam diameter to be ~55 $\mu$m and Fig. 2(h) shows the amplified seed beam with the reduced FWHM of ~15 $\mu$m (neutral density filter of 1/500 was utilized to prevent the amplified seed energy from saturating the camera). There could be two reasons for the decrease of the output seed beam size: one is the plasma focusing effect, although we did not observe the decrease in beam size if there is no pump beam. The other reason could be due to the nonlinear nature of the SRBS amplification process, since the pump is stronger in the beam center and hence the seed grows faster there.

Using the amplified pulse energy, pulse duration, and beam size given above, intensity of the amplified pulse with the maximum output energy was determined. The intensity of the pulse after single pass amplification was ~$1.3 \times 10^{16}$ W/cm$^2$ for an energy of ~1.8 mJ in the short pulse, spot size of ~15 $\mu$m, and pulse duration of ~90 fs. The input seed intensity was ~$1.3 \times 10^{12}$ W/cm$^2$ for an energy of ~16 $\mu$J, spot size of ~55 $\mu$m, and pulse duration of ~500 fs. The input pump pulse intensity, energy, spot size, and pulse duration were, respectively, ~$2.3 \times 10^{14}$ W/cm$^2$, ~90 mJ, ~50 $\mu$m, and ~20 ps. Hence, the intensity of the amplified seed pulse was increased 10 000 times, and also exceeded the pump intensity by ~50 times.

### B. The second pass

Our double-pass experimental setup was similar to that of the single pass shown in Fig. 1, except that a dichroic mirror ($M_4$) of high reflectivity at 803 nm and high transmission at 878 and 1064 nm was inserted between $M_3$ and $L_2$. Symmetrically, another dichroic mirror ($M_5$) of high reflectivity at 878 nm and high transmission at 803 and 1064 nm was inserted between $M_1$ and $L_1$. The two dichroic mirrors with high reflection at selected spectrum range allow the pump and seed to pass through for the first round of interaction, and after the first pass reflect back the amplified seed as well as the unused pump to have them interact again for a second round of amplification. The temporal synchronization between pump and seed in the first pass was adjusted by the pump delay line, and by the horizontal position of the dichroic mirror $M_4$ in the second pass.

Figures 3(a) and 3(b) show the output energy of the amplified seed in the first pass [Fig. 3(a)] and in the second pass [Fig. 3(b)] versus the temporal delay of the pump pulse. Delay "0" means that pump and seed overlap throughout the whole plasma length. For both positive and negative delays, since the pump and the seed pass part of the plasma without interacting with each other, the gain drops. Hence, the tuning range for delay also corresponds to the effective gain length. The input pump energy in the first pass was ~87 mJ and the

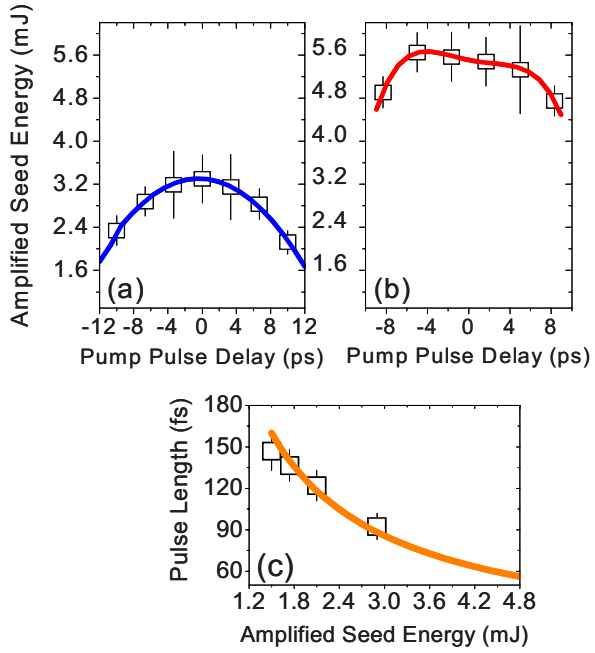


FIG. 3. (Color online) Energy gain and pulse compression in the first and second pass with the input seed energy ~16 $\mu$J. (a) The output energy in the first pass vs the pump delay time for the input pump energy ~87 mJ; and (b) the output energy in the second pass vs the pump delay time for the pump energy ~56 mJ, which takes into account the pump losses while returning to the plasma for the second pass. (c) The relationship between the output pulse width and the output energy.

input seed energy was ~16 $\mu$J. Taking into account plasma transmission of the pump beam (including pump energy transfer to the seed) and losses of the pump on optical surfaces while returning to the plasma for the second interaction, the input pump energy in the second pass was estimated to be ~56 mJ. With the maximum output energy of ~5.6 mJ, as shown in Fig. 3(b), and the maximum seed energy into the plasma for the second pass ~3.3 mJ (including losses on optics), we measured a factor of 1.7 in increase of the pulse energy after the second pass. Since the design of the second pass is, to some extent, equivalent to extending the plasma length of 2 mm in single pass to 4 mm, the factor of 1.7 in amplification in the second pass indicates that the energy of the amplified seed pulse grows almost linearly with the plasma length. As the result, in Fig. 2(a) also shows that the energy of the amplified seed pulse grows almost linearly with the pumping energy. A new parameter, which we called the "effective" gain length $L_{\text{eff}}$, might better clarify the amplification process,

$$L_{\text{eff}} = L \times E_{\text{pump}}. \tag{3}$$

Here $L$ is the plasma length and $E_{\text{pump}}$ is the pumping energy, and the amplified seed energy $E_s \propto L_{\text{eff}}$. For the first and second pass, $L_{\text{eff1}} = 2\ \text{mm} \times 87\ \text{mJ}$ and $L_{\text{eff2}} = 2\ \text{mm} \times 56\ \text{mJ}$. Therefore the amplified seed energy after the second pass $E_{s2} \propto (L_{\text{eff1}} + L_{\text{eff2}})$ and $E_{s2}/E_{s1} = (L_{\text{eff1}} + L_{\text{eff2}})/L_{\text{eff1}} = 1.6$, which agrees with the measured value of 1.7.

Figure 3(c) shows the measured output pulse width $\tau$ versus the output energy $E$. A least mean square error curve fitting of $E^a\tau = \text{const}$ indicated that $a \approx 1$, which is consistent with theoretical predictions,[9,10]

$$g_M \times \tau \sim \frac{\pi}{\sqrt{2\omega\omega_{pe}}} = \text{const}. \tag{4}$$

Here $g_M$ is the maximum vector potential of the amplified pulse, $g_M \propto (E/\tau)^{1/2}$. Using this relationship, we estimated the output pulse width after the second pass to be ~50 fs based on the obtained second pass energy of ~5.6 mJ.

## III. EXTENDING THE REGION OF RESONANCE

With the gain increase in the second pass, the energy conversion efficiency from the pump to the seed reaches ~6.4%, a factor of more than 6 improvement compared to the best of our previous results.[12]

To further improve the efficiency and performance of the system, we noticed that all our previous results were obtained in a ~2 mm plasma. As theory indicated, for a certain pump intensity and wavelength, the optimal plasma gain length is limited by instabilities such as Raman forward scattering and modulational instability. Under the condition that the plasma wave breaks near its first maximum, the optimal plasma length is given by[9,10]

$$L_{\text{amp}} \sim 0.8 z_M^{2/3} \Lambda^{1/3}. \tag{5}$$

Here, $z_M$ and $\Lambda$ are the location of the first maximum in the amplified pulse and the number of exponentiations in the instability. For pumping intensity $\sim 2 \times 10^{14}\ \text{W/cm}^2$ and pump wavelength $\lambda = 800$ nm (these are typical parameters used in the experiment), $L_{\text{amp}} \sim 3$–$6$ mm.[9]

In order to increase the plasma channel length from 2 mm to 4 mm as planned in our next set of experiments, the Rayleigh length of the ionization prepulse has to be increased by at least a factor of 2, and the prepulse energy to be doubled to keep the intensity at the same level. Additionally, in generating longer plasma, the temporal shape and spatial distribution of the prepulse might cause instabilities in the ionization process and affect the formation and longitudinal uniformity of the plasma channel. Therefore, our solution to this problem was to use two ionization pulses (two prepulses, prepulse1, and prepulse2). The foci of the two prepulse beams were adjusted and slightly separated (by ~0.5 mm) along the axis of the plasma channel.

Figures 4(a) and 4(b) show the interferogram [Fig. 4(a)] and a two-dimensional density profile [Fig. 4(b)] of the plasma channel formed by two prepulses. The interferogram and the plasma density profile were obtained using a Mach–Zehnder interferometer.[21] The two prepulses were both generated by two Nd:YAG lasers. Prepulse1 was ~10 ns with a focused spot size diameter ~65 $\mu$m and ~300 mJ beam energy and prepulse2 was ~6 ns also with a focused spot size diameter ~65 $\mu$m and ~700 mJ beam energy. The plasma was probed at a delay of ~22 ns after prepulse1 and at a delay of ~16 ns after prepulse2. It can be seen from Fig. 4 that the plasma channel has a length of ~4 mm with desired

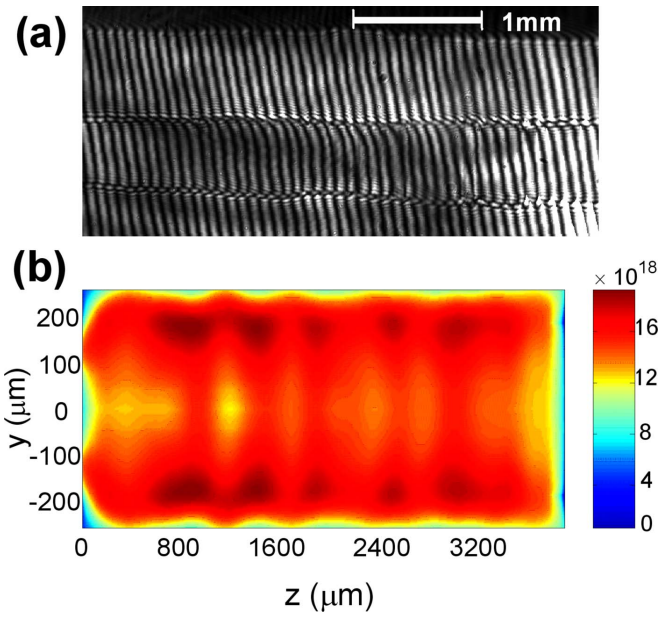


FIG. 4. (Color online) Interferogram (a) and two-dimensional density profile (b) of the ~4 mm plasma channel for SRBS amplification.

on-axis and radial density distributions, which should increase the gain length of SRBS to further improve amplification and the energy conversion efficiency.

## IV. SUMMARY

In the first pass, we demonstrated an energy amplification of >200 for a seed with input energy ~16 $\mu$J. The spectrum of the amplified pulse was broadened to ~32 nm and the pulse duration shortened to ~90 fs. The maximum unfocused intensity was $\sim 1.3 \times 10^{16}$ W/cm$^2$, which was 50 times higher than the pump intensity.

In the second pass, we demonstrated increased energy and power of output seed pulse and increased energy transfer efficiency to a level of 6.4%, without an increase in the system size. This increase of amplification and compression of output pulses provided unfocused intensity ~4 $\times 10^{16}$ W/cm$^2$ in ~50 fs, i.e., more than two orders of magnitude higher intensity than input pump intensity in the first pass.

We noticed that the obtained >6% of the energy transfer was quite noteworthy but still low compared to the theoretical prediction. We believe that the efficiency of the system can be farther increased by increasing the gain length and extend the region of resonance.

## ACKNOWLEDGMENTS

The authors are thankful to Y. Luo and S. Kheifets for their help in creating longer plasma, J. S. Wurtele, R. Lindberg, and E. J. Valeo for valuable discussions, and N. Tkach for his devoted technical support. We would also like to thank M. Shneider for helpful discussions on plasma channel.

This work was supported by NSF-MRI and DOE/NSF grants, and the NNSA under the SSAA Program through DOE Research Grant No. DE-FG52–07NA28122.

[1] E. Gerstner, Nature (London) **446**, 16 (2007).
[2] N. Patel, Nature (London) **449**, 133 (2007).
[3] M. Aoyama, K. Yamakawa, Y. Akahane, J. Ma, N. Inoue, H. Ueda, and H. Kiriyama, Opt. Lett. **28**, 1594 (2003).
[4] J. Faure, Y. Glinec, A. Pukhov, S. Kiselev, S. Gordienko, E. Lefebvre, J. P. Rousseau, F. Burgy, and V. Malka, Nature (London) **431**, 541 (2004).
[5] R. Kodama, P. A. Norreys, K. Mima, A. E. Dangor, R. G. Evans, H. Fujita, Y. Kitagawa, K. Krushelnick, T. Miyakoshi, N. Miyanaga, T. Norimatsu, S. J. Rose, T. Shozaki, K. Shigemori, A. Sunahara, M. Tampo, K. A. Tanaka, Y. Toyama, Y. Yamanaka, and M. Zepf, Nature (London) **412**, 798 (2001).
[6] D. V. Korobkin, C. H. Nam, S. Suckewer, and A. Golsov, Phys. Rev. Lett. **77**, 5206 (1996).
[7] Y. Glinec, J. Faure, V. Malka, T. Fuchs, H. Szymanowski, and U. Oelfke, Med. Phys. **33**, 155 (2006).
[8] D. Strickland and G. Mourou, Opt. Commun. **56**, 219 (1985).
[9] V. M. Malkin, G. Shvets, and N. J. Fisch, Phys. Rev. Lett. **82**, 4448 (1999).
[10] N. J. Fisch and V. M. Malkin, Phys. Plasmas **10**, 2056 (2003); V. M. Malkin and N. J. Fisch, *ibid.* **12**, 044507 (2005).
[11] Y. Ping, W. Cheng, S. Suckewer, D. S. Clark, and N. J. Fisch, Phys. Rev. Lett. **92**, 175007 (2004).
[12] W. Cheng, Y. Avitzour, Y. Ping, S. Suckewer, N. J. Fisch, M. S. Hur, and J. S. Wurtele, Phys. Rev. Lett. **94**, 045003 (2005).
[13] M. Dreher, E. Takahashi, J. Meyer-ter-Vehn, and K. Witte, Phys. Rev. Lett. **93**, 095001 (2004).
[14] R. K. Kirkwood, E. Dewald, C. Niemann, N. Meezan, S. C. Wilks, D. W. Price, O. L. Landen, J. Wurtele, A. E. Charman, R. Lindberg, N. J. Fisch, V. M. Malkin, and E. O. Valeo, Phys. Plasmas **14**, 113109 (2007).
[15] D. S. Clark and N. J. Fisch, Phys. Plasmas **10**, 3363 (2003); **10**, 4837 (2003).
[16] V. M. Malkin, G. Shvets, and N. J. Fisch, Phys. Plasmas **7**, 2232 (2000).
[17] P. Mardahl, H. J. Lee, G. Penn, J. S. Wurtele, and N. J. Fisch, Phys. Lett. A **296**, 109 (2002); I. Y. Dodin, G. M. Fraiman, V. M. Malkin, and N. J. Fisch, J. Exp. Theor. Phys. **95**, 625 (2002).
[18] V. M. Malkin, G. Shvets, and N. J. Fisch, Phys. Rev. Lett. **84**, 1208 (2000).
[19] N. A. Yampolsky, N. J. Fisch, S. Li, V. Malkin, A. Morozov, J. Ren, S. Suckewer, E. Valeo, R. Lindberg, and J. Wurtele, Bull. Am. Phys. Soc. **52**, 82 (2007).
[20] J. Ren, W. Cheng, S. Li, and S. Suckewer, Nat. Phys. **3**, 732 (2007).
[21] Y. Ping, I. Geltner, A. Morozov, and S. Suckewer, Phys. Plasmas **9**, 4756 (2002).